PRAMANA
— journal of
physics

Vol. 74, No. 4
April 2010
pp. 525–539

Structure of negative parity yrast bands in odd mass $^{125-131}$Ce nuclei

ARUN BHARTI*, SURAM SINGH and S K KHOSA
Department of Physics and Electronics, University of Jammu, Jammu 180 006, India
*Corresponding author. E-mail: arunbharti_2003@yahoo.co.in

MS received 21 July 2009; revised 20 November 2009; accepted 22 December 2009

Abstract. The negative parity yrast bands of neutron-deficient $^{125-131}$Ce nuclei are studied by using the projected shell model approach. Energy levels, transition energies and $B(M1)/B(E2)$ ratios are calculated and compared with the available experimental data. The calculations reproduce the band-head spins of negative parity yrast bands and indicate the multi-quasiparticle structure for these bands.

Keywords. Projected shell model; band diagrams; transition energies; $B(M1)/B(E2)$ ratios.

PACS Nos 21.60.Cs; 21.10.Ky; 21.10.Re; 27.60.+j

1. Introduction

Neutron-deficient nuclei in the light-rare-earth region with $A \approx 130$ lie in the region close to the $N = 82$ shell gap and have been the subject of many experimental studies as these nuclei exhibit a competition between spherical and deformed shapes. Light neutron-deficient odd-neutron cerium isotopes with $A \approx 130$ can be cited as one such example which are currently of interest in high-spin nuclear structure physics because they are well deformed with a quadrupole deformation of $\beta_2 = 0.25$–0.30 [1]. Consequently, γ-ray spectroscopy of these nuclei is dominated by rotational bands, built on the ground and low-lying excited states. The behaviour of these rotational bands can provide useful information about the underlying nuclear structure. The ^{125}Ce nucleus is the lightest even–odd isotope of which the band structures have been published by Paul *et al* [2]. Excited states in ^{125}Ce have been extensively studied up to very high spins in recent years [3,4]. These studies, however, vary in the assignments for the spins, parities and relative excitation energies of the single-quasiparticle intrinsic states. Multiple bands have been reported to exist in ^{125}Ce by these studies. However, the negative parity band is lower in energy than the other bands. This negative parity band is based on a $7/2^-$ state and was assigned to ^{125}Ce on the basis of the coincidence between the γ-rays and $A = 125$ recoils detected at the focal plane of a recoil mass separator.

No γ-rays connecting this band with other bands were observed. In the heavier ^{127}Ce nucleus [5,6] three bands were identified: two based on $5/2^+$ and $7/2^-$ states as in ^{125}Ce, separated by an excitation energy estimated to be lower than 20 keV [6], and one based on a $1/2^+$ state, which is also present in the heavier ^{129,131,133}Ce nuclei [7,8]. Apparently, the excitation energy of the $7/2^-$ state with respect to the $5/2^+$ state decreases with decreasing neutron number. The ground state of the lighter Ce isotopes have spin $7/2^-$ and not $5/2^+$ as proposed previously [6]. The odd-neutron isotopes ^{129}Ce and ^{131}Ce have been studied by Gizon *et al* [9], who established decay schemes for both positive and negative parity states and made spin and multipolarity assignments from angular distribution measurements. Aryaeinejad *et al* [10] have reported decay scheme of ^{129}Ce for both positive and negative parity states and extended the previously known [9] states with the addition of five new high-spin positive parity levels [$J^\pi = 23/2^+ - 31/2^+$] and seven new high-spin negative parity levels [$J^\pi = 25/2^- - 39/2^-$]. Sometime back, Galindo-Uribarri *et al* [11] have extended the level structure of ^{129}Ce further to high spin for both positive and negative parity states (up to $J^\pi = 73/2^+$ and $J^\pi = 55/2^-$). It turns out that in ^{129}Ce, there is a negative parity band with band head $7/2^-$ similar to the negative parity band that exists in $^{125-127}$Ce but is higher in energy than the $5/2^+$ positive parity band. Further, the negative parity band in ^{131}Ce close to the ground state band has a band head $9/2^-$ [7].

In recent years, the projected shell model (PSM) [12] has become quite successful in explaining a broad range of properties of deformed nuclei in various regions of nuclear periodic table. The most striking aspect of this quantum mechanical model is its ability to describe the finer details of high-spin spectroscopy data with simple physical interpretations. The advantage of this method is that the numerical requirement is minimal. The PSM approach is based on the diagonalization in the angular momentum projected basis from the deformed Nilsson states. The PSM has been systematically applied to study the rare-earth nuclei [13,14] and the agreement between the PSM results and experimental data has been found to be quite good.

The purpose of the present work is to interpret the negative parity bands observed in $^{125-131}$Ce in the framework of PSM and also to test the applicability of this model for odd mass in the $A = 120$–130 mass region. In the present study, the results are obtained for the energy spectrum, transition energies and $B(M1)/B(E2)$ ratios. Previously, PSM has been successfully applied to study the even–even $^{122-130}$Ce nuclei [15–17].

The paper is organized as follows: In §2, we shall give an outline of the PSM approach. The results of calculations and comparisons with the experimental data are presented in §3. Finally, the conclusions drawn from the present analysis are given in §4.

2. Projected shell model

The detailed theory of PSM is given in [12]. In this section, we give a brief outline of PSM. For the present study, we include 1- and 3-quasiparticle (qp) states $|\phi_\kappa\rangle$ as

$$|\phi_\kappa\rangle = \{\alpha_\nu^\dagger|o\rangle, \alpha_\nu^\dagger\alpha_{\pi 1}^\dagger\alpha_{\pi 2}^\dagger|o\rangle\} \tag{1}$$

for odd-neutron nuclei, where $\alpha^\dagger$'s are the quasipartcle (qp) creation operators, ν's (π's) denote the neutron (proton) Nilsson quantum numbers which run over low-lying orbitals and $|o\rangle$ is the Nilsson+BCS vacuum (o-qp state). In eq. (1), the low-lying 3-qp states selected for the many-body basis are those consisting of 1-qp plus a pair of qp's from nucleons of another kind. This selection is based on physical considerations. In general, 3-qp states made by three nucleons of the same kind are also allowed, but such states usually lie in higher energy region.

The many-body wave function is a superposition of projected (angular momentum) multi-quasiparticle states,

$$|\sigma, IM\rangle = \sum_{K,\kappa} f_\kappa^{\sigma,I} \hat{P}^I_{MK} |\phi_\kappa\rangle = \sum_\kappa f_\kappa^{\sigma,I} \hat{P}^I_{MK\kappa} |\phi_\kappa\rangle, \tag{2}$$

where σ labels the states with same angular momentum and κ is the basis state. $\hat{P}^I_{MK}$ is the angular momentum projection operator which projects the quantum numbers I, M and is defined as

$$\hat{P}^I_{MK} = \frac{I+1/2}{4\pi^2} \int \mathrm{d}\Omega \hat{R}(\Omega) D^{I*}_{MK}(\Omega),$$

where $\hat{R}(\Omega)$ is the rotational operator, $D^{I*}_{MK}(\Omega)$ is the D function (irreducible representation of the rotation group) and Ω is the Euler angle. $f_\kappa^{\sigma,I}$ are the weights of the basis states κ. Since we have assumed axial symmetry for the basis states, the intrinsic states $|\phi_\kappa\rangle$ have a good K quantum number, K_κ. Axial symmetry implies that the set of quantum numbers κ contains, among other things, the total intrinsic magnetic quantum number K implicitly. We can, therefore, omit writing K in the weight coefficients $f_\kappa^{\sigma,I}$ for such a system. Moreover, the summations over K may also be omitted, since only one specific K contributes to the sum for a given κ. Since the axial symmetry is kept for Nilsson states, K is a good quantum number. It can be used to label the basis states in eq. (1).

The weight factors $f_\kappa^{\sigma,I}$ in eq. (2) are determined by the diagonalization of the shell model Hamiltonian in the space spanned by the projected basis states given above. This leads to the eigenvalue equation (for a given spin I) which is given by

$$\sum_{\kappa'} (H^I_{\kappa\kappa'} - E_{\sigma,I} N_{\kappa\kappa'}) f_{\kappa'}^{\sigma,I} = 0,$$

and the normalization is chosen such that

$$\sum_{\kappa\kappa'} f_\kappa^{\sigma,I} N_{\kappa\kappa'} f_{\kappa'}^{\sigma',I'} = \delta_{\sigma\sigma'}\delta_{II'},$$

where the Hamiltonian and norm matrix elements are defined by

$$H_{\kappa\kappa'} = \langle\phi_\kappa|\hat{H}\hat{P}^I_{K_\kappa K'_{\kappa'}}|\phi_{\kappa'}\rangle$$

and

$$N_{\kappa\kappa'} = \langle\phi_\kappa|\hat{P}^I_{K_\kappa K'_{\kappa'}}|\phi_{\kappa'}\rangle.$$

Projecting an intrinsic state $|\phi_\kappa\rangle$ onto a good angular momentum generates the rotational band associated with this intrinsic configuration, whose rotational energy is given by the expectation value of the Hamiltonian as a function of spin I. That is,

$$E_\kappa(I) = \frac{\langle\phi_\kappa|\hat{H}\hat{P}^I_{KK}|\phi_\kappa\rangle}{\langle\phi_\kappa|\hat{P}^I_{KK}|\phi_\kappa\rangle} = \frac{H_{\kappa\kappa}}{N_{\kappa\kappa}}.$$

It represents the expectation value of the Hamiltonian with respect to a projected quasiparticle state κ. A diagram in which rotational energies of various bands are plotted against the spin (I) will be referred to as a band diagram which contains incredibly rich information.

The usual separable force Hamiltonian [12]

$$\hat{H} = \hat{H}_0 - \frac{\chi}{2}\sum_\mu \hat{Q}^\dagger_\mu \hat{Q}_\mu - G_M \hat{P}^\dagger \hat{P} - G_Q \sum_\mu \hat{P}^\dagger_\mu \hat{P}_\mu, \tag{3}$$

has been used successfully to explain the system of rotational spectra for a large number of nuclei. The first term is the spherical single-particle Hamiltonian

$$\hat{H}_0 = \sum_\alpha c^\dagger_\alpha E_\alpha c_\alpha, \tag{4}$$

where $c^\dagger_\alpha$ and c_α are the single-particle creation and annihilation operators respectively, and E_α is the single-particle energy given by

$$E_\alpha = \hbar\omega[N - 2\kappa\hat{l}\cdot\hat{s} - \kappa\mu(\hat{l}^2 - \langle\hat{l}\rangle^2)], \tag{5}$$

where ω is the harmonic-oscillator parameter which incorporates the principle of volume conservation for nuclei deformed from spherical shapes, s and l represent the intrinsic nucleon spins and orbital angular momenta in the stretched coordinate basis. The Nilsson parameters κ and μ are taken from the N-dependent values of [18,19]. The remaining terms in eq. (3) are the residual quadrupole–quadrupole, the monopole pairing and the quadrupole pairing interactions, respectively. The strength χ of the quadrupole–quadrupole term can be obtained via self-consistent conditions with a given deformation parameter, β_2. The present calculations are performed by considering three major shells ($N = 3$, 4 and 5) for both protons and neutrons. The basis deformation β_2 is taken from ref. [20] as $\beta_2 = 0.31$ for both ^{125}Ce and ^{127}Ce nuclei and it is 0.28, 0.23 for ^{129}Ce, ^{131}Ce respectively.

The operators appearing in eq. (3) are defined as [12]

$$\hat{Q}_\mu = \sum_{\alpha\beta} c^\dagger_\alpha (Q_\mu)_{\alpha\beta} c_\beta,$$

$$(Q_\mu)_{\alpha\alpha'} = \sqrt{\frac{4\pi}{5}}\delta_{NN'}\langle Njm|\left(\frac{r}{b}\right)^2 Y_{2\mu}|N'j'm'\rangle,$$

where

$$|\alpha\rangle = |Njm\rangle \quad \text{and} \quad |\alpha'\rangle = |N'j'm'\rangle.$$

$$\hat{P}^{\dagger} = \frac{1}{2}\sum_{\alpha} c_{\alpha}^{\dagger} c_{\bar{\alpha}}^{\dagger},$$

$$\hat{P}_{\mu}^{\dagger} = \frac{1}{2}\sum_{\alpha\beta} c_{\alpha}^{\dagger} (Q_{\mu})_{\alpha\beta} c_{\bar{\beta}}^{\dagger}.$$

The strength of the quadrupole–quadrupole force was adjusted such that the known (input) quadrupole deformation (β_2) is obtained as a result of the self-consistent interactions given by

$$G_M = \left(G_1 - G_2 \frac{N-Z}{A}\right) \frac{1}{A}(\text{MeV}), \tag{6}$$

$$G_Q = \gamma G_M(\text{MeV}), \tag{7}$$

where G_M is inversely proportional to the particle number A and contains two adjustable constants G_2 and G_1. Adjusting the parameter β_2, G_2 and G_1 will change the energy gap for each shell and thus will affect the selection of the quasiparticle basis. In our calculations G_1 is taken as 21.40 for both neutrons and protons and G_2 is taken as 13.13 (0) for neutrons (protons). The strength of the quadrupole-quadrupole pairing force, G_Q, is assumed to be proportional to G_M. One may carefully adjust the ratio of G_Q/G_M during the calculations to get the best overall agreement with the experimental data. In the present calculations, the ratio of G_Q/G_M is fixed as 0.18 which is the same as taken by Hara and Sun [12,13] for the PSM calculations of the lighter part of rare-earth region. After diagonalizing the Hamiltonian in the quasiparticle basis, the lowest energy for each spin is used to compare with the experimental yrast energy.

3. Results and discussion

3.1 *Yrast spectra in $^{125-131}Ce$*

In figures 1a–1d, we present the yrast spectra of $^{125-131}$Ce isotopes. The theoretical spectra have been obtained for that value of quadrupole deformation for which the potential energy surface (PES) of the band-head shows a minimum. In the case of ^{125}Ce, theoretical yrast spectra match with the experimental values for spin values up to $21/2^{-}\hbar$. For spins higher than this value, the theoretical values up to spin $45/2^{-}\hbar$ are slightly higher than the experimental values. The quadrupole deformation parameter (β_2) for which the theoretical results are obtained for ^{125}Ce is 0.295, which is very close to the observed experimental value of 0.31. In ^{127}Ce, the theoretical values are observed to be higher than the experimentally observed values but nevertheless very close to the experimental values up to a spin of $19/2^{-}$ $\hbar$. After that, the values disagree with the theoretical results. This difference between the theoretical values remains constant for the spins ranging from $31/2^{-}\hbar$ to $51/2^{-}\hbar$.

The theoretical values all along are found to be higher than the experimentally observed yrast energies. For ^{127}Ce, the theoretical yrast spectra have been obtained for a quadrupole deformation of $\beta_2 = 0.295$, which is again found to be matching with the experimental value of 0.31. Similar agreement is obtained for ^{129}Ce and ^{131}Ce. In ^{129}Ce, the agreement between theoretical and experimental values is very good for spin values up to $17/2^{-}\hbar$ whereas after this, the disagreement increases with the increase in the spin. The difference between theoretical and experimental values becomes nearly constant beyond the spin value of $29/2^{-}\hbar$. Similar features are observed in ^{131}Ce. The quadrupole deformation parameters for which the theoretical calculation was made are 0.275 and 0.22 for ^{129}Ce and ^{131}Ce respectively. These values are also in reasonable agreement with the experimentally observed quadrupole deformation values of 0.28 and 0.23 for ^{129}Ce and ^{131}Ce respectively.

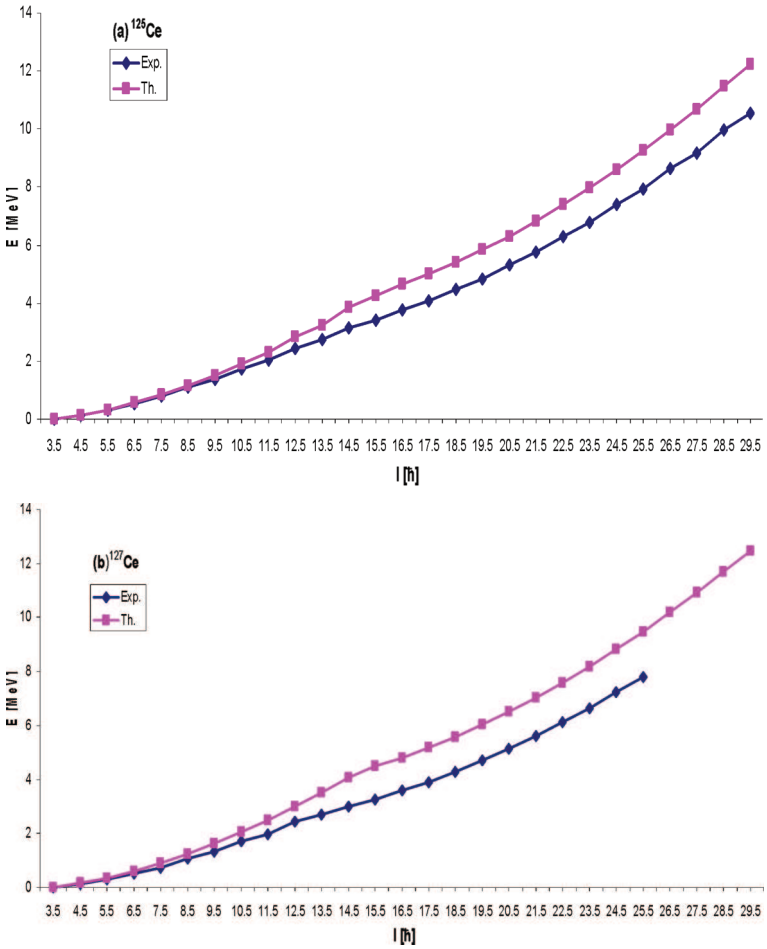

Figures 1a–1b.

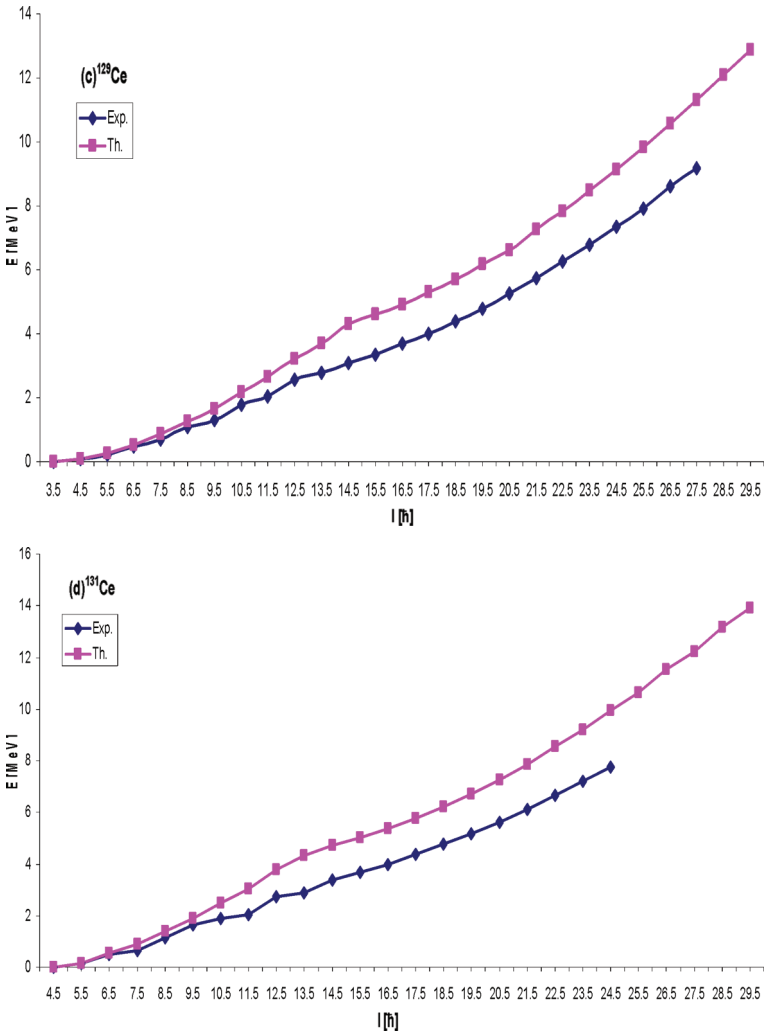

Figure 1. Comparison of calculated (th.) yrast spectra with the experimental (expt.) data for (**a**) ^{125}Ce [4], (**b**) ^{127}Ce [26], (**c**) ^{129}Ce [11] and (**d**) ^{131}Ce [27].

3.2 *Transition energy versus spin*

In figures 2a–2d, we present the plots of transition energy $E(I) - E(I-1)$ vs. spin (I) for $^{125-131}$Ce isotopes obtained for prolate deformation. It may be noted that in the case of ^{125}Ce, variations shown by calculated transition energies with spin agree qualitatively with the experimental changes up to the spin value of $53/2^{-}\hbar$. The calculated results for the transition energies all along are found to be higher than the experimental values. In the case of ^{127}Ce, the calculated transition plot shows agreement with the experimental plot for spins ranging from $9/2^{-}\hbar$ to $13/2^{-}\hbar$ and from $33/2^{-}\hbar$ to $49/2^{-}\hbar$. However, in the spin range of $15/2^{-}\hbar$ to $31/2^{-}\hbar$, the

variations in the transition energies are not reproduced. Further, it may be noted that for the entire spin range, the calculated transition energy values are higher than the experimentally measured values. In the case of ^{129}Ce, the calculated results are obtained up to the spin range of $59/2^{-}\hbar$ whereas the experimental values are available from $9/2^{-}\hbar$ to $55/2^{-}\hbar$. Note that, the calculated values of transition energy show similar trend for spin values above $21/2^{-}\hbar$. For spin values around $27/2^{-}\hbar$, the experimental transition energies show an increasing trend on either side of the spin of $27/2^{-}\hbar$. This feature is very well reproduced qualitatively by the calculated transition energy values. Besides this, the transition energies for the spin range $9/2^{-}\hbar$–$13/2^{-}\hbar$ are also reproduced. However, the variation in the observed transition energies in the spin range $15/2^{-}\hbar$–$19/2^{-}\hbar$ are not satisfactorily reproduced in ^{129}Ce.

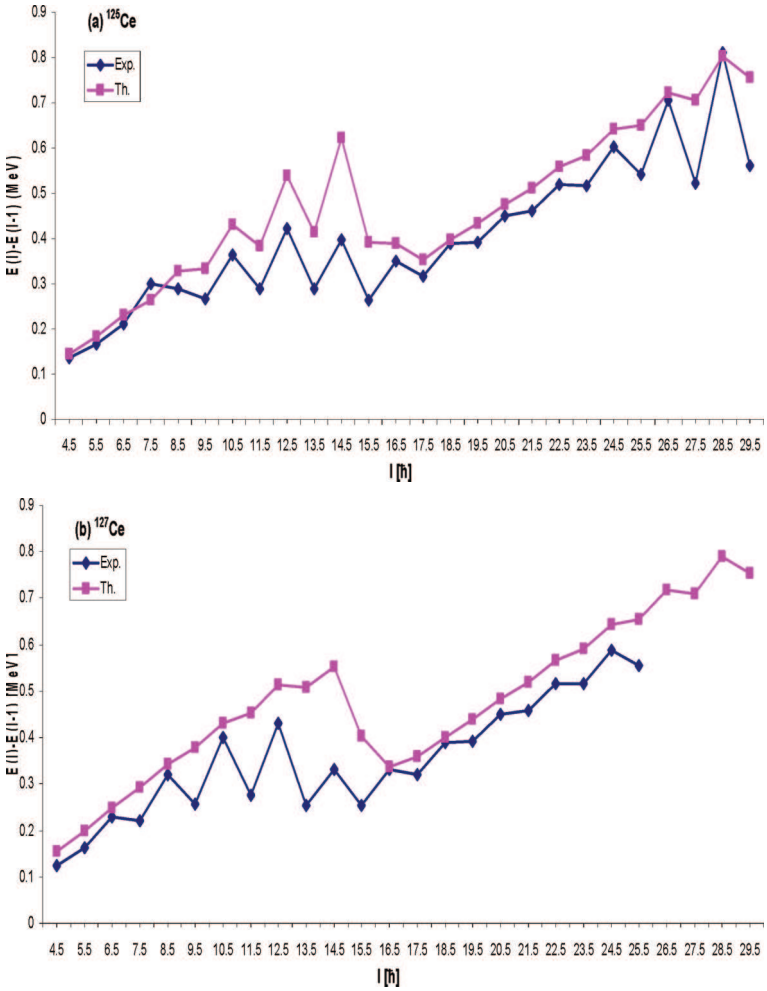

Figures 2a–2b.

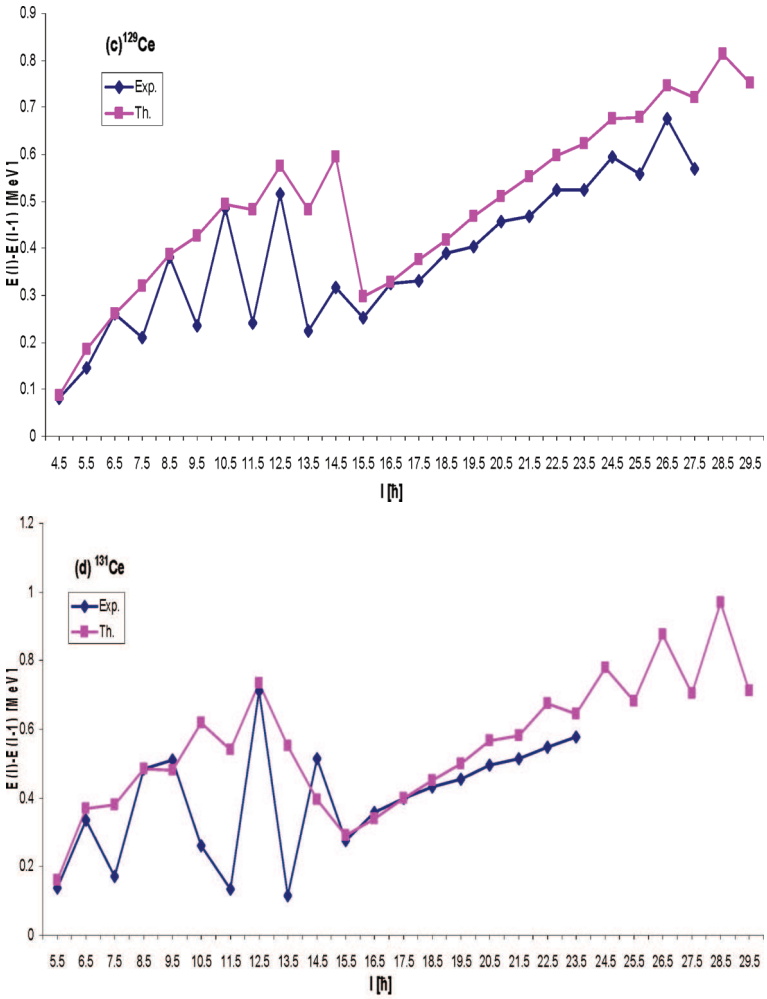

Figure 2. Comparison of calculated (squares) and experimental (diamond) transition energies $E(I) - E(I-1)$ vs. spin (I) for (**a**) ^{125}Ce, (**b**) ^{127}Ce, (**c**) ^{129}Ce and (**d**) ^{131}Ce nuclei.

For ^{131}Ce, one notes a good agreement between experimental and theoretical values of the transition energy for the spins ranging from $11/2^-\hbar$ to $19/2^-\hbar$ and from $31/2^-\hbar$ to $45/2^-\hbar$. However, for the spin range of $21/2^-\hbar$–$29/2^-\hbar$, the calculated results do not satisfactorily reproduce the observed values of transition energies. For this nucleus, the transition energies are calculated up to the spin of $59/2^-\hbar$.

From the presentation of results on transition energy, one notices that the experimental data show strong staggering in figures 2a–d and the calculated numbers do not match with these except to a good extent in figure 2a. This type of agreement could be because of the truncation effects of the basis and limitation of the phenomenological two-body residual interaction employed in the present calculation.

It is well known that transition energy data are physical quantity which depend very sensitively on the type of two-body residual interaction as well as truncation of the basis states.

We notice here the interesting phenomenon that the band-head spin of the nuclei $^{125-129}$Ce is $7/2^-$ while that of the neighbouring nucleus ^{131}Ce is $9/2^-$. This means that when two more neutrons are added to ^{129}Ce, there occurs a sudden change of the band-head spin.

3.3 *Band diagram of* $^{125-131}$*Ce*

In figures 3a–3d, we present the band diagrams for $^{125-131}$Ce isotopes. From the band diagram of ^{125}Ce (see figure 3a), it is observed that the energy states from $7/2^-\hbar$ to $27/2^-\hbar$ of the yrast band arise from one 1-qp neutron state $1\nu h_{11/2}[-7/2]K = -7/2$. Then, between $27/2^-$ and $33/2^-$ spins, it is found that two 1-qp neutron states, $1\nu h_{11/2}[5/2]K = 5/2$ and $1\nu h_{11/2}[-7/2]K = -7/2$, merge together and therefore, these states arise from a superposition of these bands. Then, these bands are crossed by 3-qp band with configuration $1\nu h_{11/2}[-7/2] + 2\pi h_{11/2}[1/2, -3/2]K = -9/2$ and also by 3-qp band with configuration $1\nu h_{11/2}[-7/2] + 2\pi h_{11/2}[-3/2, 5/2]K = -5/2$. The angular momentum states higher than $33/2^-\hbar$ arise from these two bands which are almost having competing energies for spins greater than $33/2^-\hbar$.

In figure 3b, we present the band diagrams for ^{127}Ce. For ^{127}Ce, it is observed that the yrast states starting from $7/2^-\hbar$ to $33/2^-\hbar$ arise from one 1-qp neutron band $1\nu h_{11/2}[-7/2]K = -7/2$. After $33/2^-\hbar$, this band is crossed by three distinct bands having competing energies. The higher states of ^{127}Ce would, therefore, be thought to be arising from these four 3-qp bands which have the following configurations:

$$1\nu h_{11/2}[-7/2] + 2\pi h_{11/2}[1/2, -3/2]K = -9/2,$$

$$1\nu h_{11/2}[-7/2] + 2\pi h_{11/2}[-3/2, 5/2]K = -5/2,$$

$$1\nu h_{11/2}[-7/2] + 2\pi h_{11/2}[1/2, -3/2]K = 5/2$$

and

$$1\nu h_{11/2}[-7/2] + 2\pi h_{11/2}[-3/2, 5/2]K = 9/2.$$

Now coming to the discussion on ^{129}Ce. The band diagrams for ^{129}Ce are presented in figure 3c. Here, one notices that the yrast states up to the spin value of $31/2^-\hbar$ arise from one 1-qp neutron band $1\nu h_{11/2}[-7/2]K = -7/2$. Thereafter, this band is crossed by three 3-qp distinct bands having configurations

$$1\nu h_{11/2}[-7/2] + 2\pi h_{11/2}[1/2, -3/2]K = -9/2,$$

$$1\nu h_{11/2}[-7/2] + 2\pi h_{11/2}[-3/2, 5/2]K = -5/2$$

and

$$1\nu h_{11/2}[-7/2] + 2\pi h_{11/2}[-3/2, 5/2]K = 9/2.$$

Now for ^{131}Ce (see figure 3d), it is observed that the band-head starts for $J^{\pi} = 9/2^{-}\hbar$ whereas in the other isotopes discussed earlier, it started from $J^{\pi} = 7/2^{-}\hbar$. Further, it is noted that the yrast states from $9/2^{-}\hbar$ to $13/2^{-}\hbar$ arise from one 1-qp neutron $1\nu h_{11/2}[9/2]K = 9/2$ band. From $15/2^{-}\hbar$–$27/2^{-}\hbar$, the yrast states arise from one 1-qp neutron $1\nu h_{11/2}[-7/2]K = -7/2$ band. This band after $27/2^{-}\hbar$ is crossed by the two bands which have nearly overlapping energy. This makes us draw the inference that the yrast states with spin greater than $27/2^{-}\hbar$ arise from these two 3-qp bands having configurations, $1\nu h_{11/2}[-7/2]+2\pi h_{11/2}[1/2, -3/2]K = -9/2$ and $1\nu h_{11/2}[-7/2]+2\pi h_{11/2}[1/2, 3/2]K = 5/2$. From the discussion presented

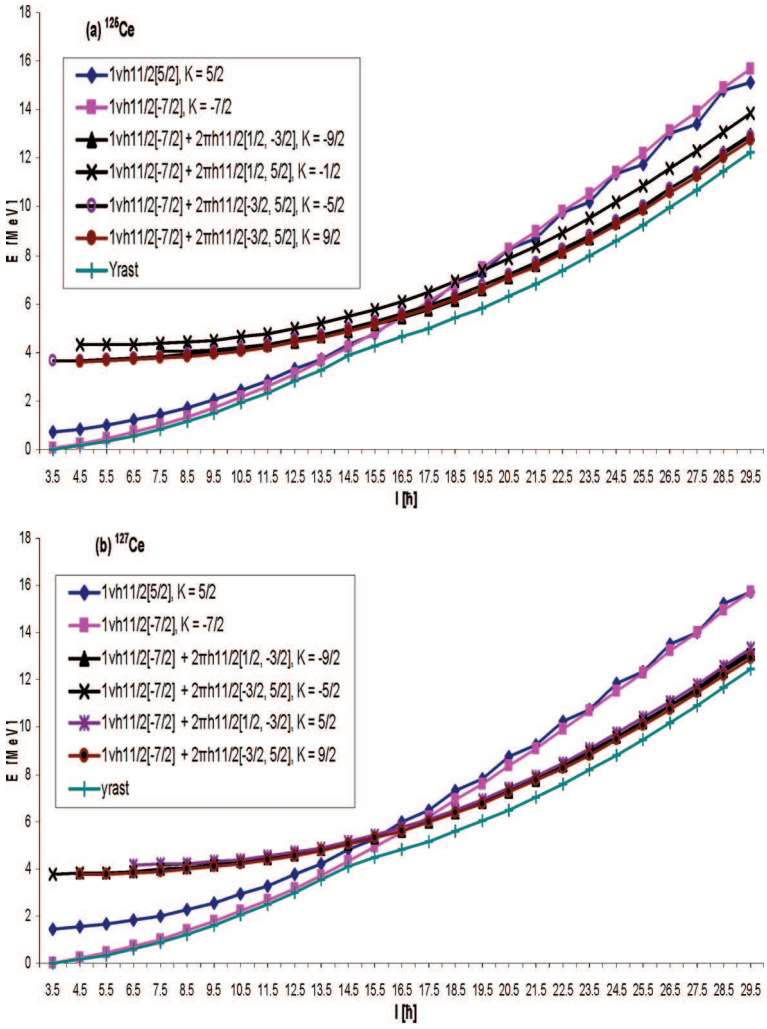

Figures 3a–3b.

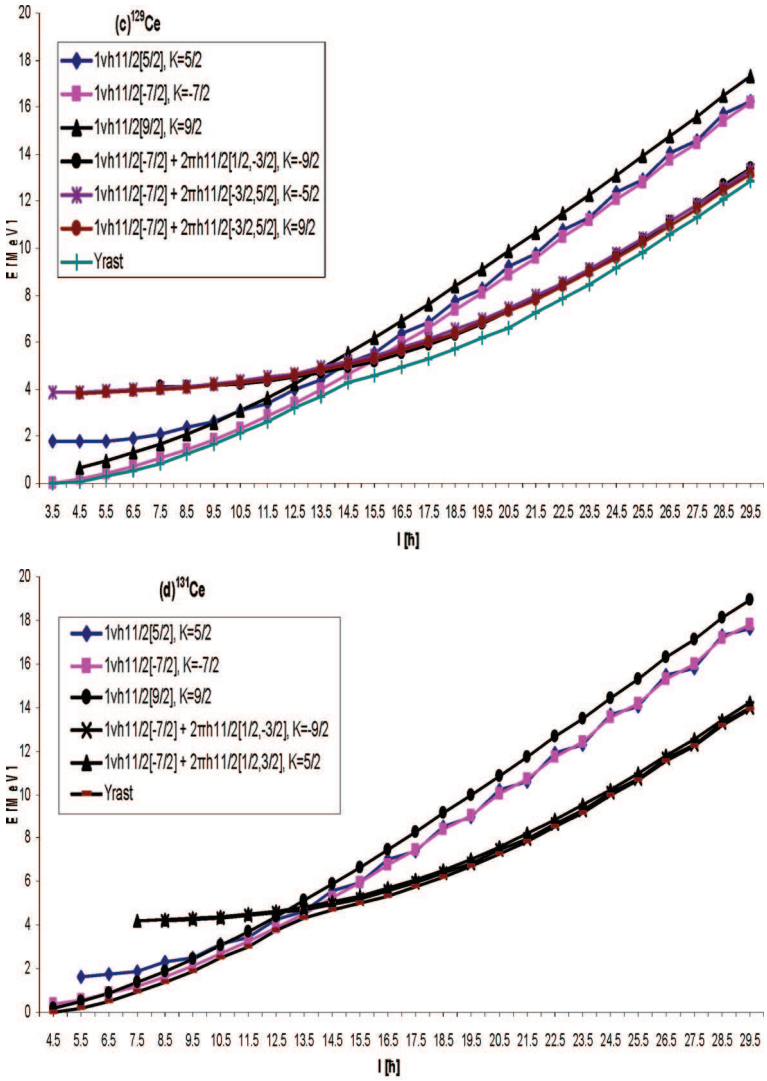

Figure 3. Band diagrams for (**a**) ^{125}Ce, (**b**) ^{127}Ce, (**c**) ^{129}Ce, (**d**) ^{131}Ce nuclei. Only the important lowest lying bands in each configuration are shown.

in the band diagram, it is very clear that the low-lying yrast spectra in $^{125-131}$Ce arise from a single band whereas the higher angular momentum states could to be thought to be arising from a superposition of bands having different configurations which means that there is a strong possibility of observing co-existence of shapes in $^{125-131}$Ce at higher spins. The change of band-head energy as we go from ^{129}Ce to ^{131}Ce could be attributed to the crossing of two 1-qp bands having configurations $1h_{11/2}[K = -7/2]$ and $1h_{11/2}[K = 9/2]$ with $K = 9/2$ band being lower.

3.4 *Transition strength $B(M1)/B(E2)$ ratios*

The ratios of the reduced transition probabilities $B(M1)/B(E2)$ give very important information about the underlying structure of a rotational band. These values are strongly dependent upon the occupied orbitals and therefore, a comparison between observed values and the values predicted by the theory can help to identify the quasiparticle configuration and serve as a test of the theoretical framework. We have obtained the $B(M1)/B(E2)$ ratios by using the following equations:

$$B(E2) = e^2 Q_0^2 \frac{15}{32\pi} \frac{(I-1-K)(I-1+K)(I-K)(I+K)}{(I-1)(2I-1)I(2I+1)} \tag{8}$$

$$B(M1) = \frac{3}{4\pi}(g_{\mathrm{k}} - g_{\mathrm{R}})^2 \mu_N^2 K^2 \frac{(I+1-K)(I+1+K)}{(I+1)(2I+3)}. \tag{9}$$

These formulae were also used for similar calculations by Vogel *et al* [21]. In the above eq. (9), the parameter g_{R} is the rotational gyromagnetic factor and the standard approximation of $g_{\mathrm{R}} = Z/A$ has been used in literature. However, this approximate value of g_{R} has often been modified by a factor of 0.7 to better fit experimental data [22]. In the present work, we have modified g_{R} by a factor of 0.85. The g_{k} parameters are the orbital gyromagnetic factors. We have used the value $g_{\mathrm{k}} = -0.21$ [23] as it was used to calculate the Dönau and Frauendorf estimates of $B(M1)/B(E2)$ ratios [24,25] in ^{125}Ce.

In table 1, we present the calculated results on transition strength $B(M1)/B(E2)$ ratios for $^{125-131}$Ce. These ratios are calculated along the spin $11/2^-$ to $35/2^-$. The experimental values are only available for ^{125}Ce. It is clear from table 1 that the agreement between the experimental and the theoretical values is reasonable up to a spin of $35/2^-\hbar$ for ^{125}Ce. For example, the calculated ratio for the spin value of $11/2^-\hbar$ comes out to be 2.03 units whereas its experimental value is 1.69 ± 0.04 units. The calculated value at spin $29/2^-\hbar$ is 0.65 units whereas the experimental value is 0.73 ± 0.05 units. The theoretical values for the transition strength ratios show a similar trend as is shown by the experimental values as we move from spin $11/2^-\hbar$ to $31/2^-\hbar$. Hereafter, the experimental values are observed to increase whereas the calculated values remain constant.

The calculated results for $^{127-131}$Ce show a similar trend as is shown for ^{125}Ce. However, no comment can be made about their agreement with the experimental data as experimental data are not available for these nuclei.

4. Conclusions

The projected shell model calculations carried out for $^{125-131}$Ce isotopes show satisfactory agreement with the observed yrast spectra. The calculated values of yrast energies are all along higher than the observed negative parity yrast energies for $^{125-131}$Ce. The calculations reproduce the band-head spin of $^{125-129}$Ce nuclei, which turns out to be $7/2^-$ for them while for the neighbouring ^{131}Ce isotope, this turns out to be $9/2^-$. This result has also been experimentally corroborated

Table 1. Comparison of experimental (expt.) and calculated (th.) transition strength $B(M1)/B(E2)$ ratios (in units of $(\mu_N/\text{eb})^2$) for ^{125,127,129,131}Ce.

	$B(M1)/B(E2)$ $(\mu_N/\text{eb})^2$				
	^{125}Ce		^{127}Ce	^{129}Ce	^{131}Ce
Spin	Th.	Expt.[a]	(Th.)[b]	(Th.)[b]	(Th.)[b]
$11/2^-$	2.03	1.69(4)	1.94	2.28	–
$13/2^-$	1.21	1.11(2)	1.16	1.37	6.47
$15/2^-$	0.96	0.92(3)	0.93	1.09	3.70
$17/2^-$	0.85	1.66(5)	0.82	0.96	2.85
$19/2^-$	0.79	0.93(3)	0.75	0.88	2.46
$21/2^-$	0.74	0.74(4)	0.71	0.84	2.24
$23/2^-$	0.72	0.87(7)	0.69	0.80	2.09
$25/2^-$	0.70	–	0.67	0.78	1.99
$27/2^-$	0.68	–	0.65	0.76	1.92
$29/2^-$	0.67	0.73(5)	0.64	0.75	1.87
$31/2^-$	0.66	0.40(1)	0.63	0.74	1.83
$33/2^-$	0.65	2.10(1)	0.63	0.73	1.80
$35/2^-$	0.65	1.27(9)	0.62	0.73	1.77

[a]Expt. data taken from ref. [4].

[b]Expt. data not available.

by Gizon *et al* [7]. From the results of band diagram, it is established that the yrast negative parity states do not arise from a single band. They arise from one-quasiparticle (1-qp) or three-quasiparticle (3-qp) bands. Besides this, the results suggest that the low-lying yrast spectra of $^{125-131}$Ce arise from a single band whereas the higher angular momentum states could be thought to be arising from a superposition of bands which indicates the possibility of co-existence of shapes in $^{125-131}$Ce at higher spins. The calculations also make a prediction of transition strength $B(M1)/B(E2)$ ratios for $^{127-131}$Ce. The experimental values for these nuclei have as yet not been measured.

Acknowledgements

The authors would like to thank Dr Y Sun and Dr J A Sheikh for making us available the code of PSM through Dr J A Sheikh.

References

[1] P Möller, J R Nix, W D Myers and W J Swiatecki, *At. Data Nucl. Data Tables* **59**, 185 (1995)
[2] E S Paul *et al*, *Phys. Rev.* **C58**, 801 (1998)
[3] C M Petrache *et al*, *Eur. Phys. J.* **A14**, 439 (2002)

[4] J F Smith *et al*, *Phys. Rev.* **C69**, 034339 (2004)
[5] B M Nyako, J Gizon, V Barci, A Gizon, S Andre, D Barneoud, D Curien, J Genevey and J C Merdinger, *Z. Phys.* **A334**, 513 (1989)
[6] A Gizon, J Genevey, D Barneoud, A Astier, R Beraud, Gh Cata-Danil, A Emsallem, J Gizon, Y Le Coz, C F Liang and P Paris, *Z. Phys.* **A351**, 361 (1995)
[7] A Gizon *et al*, *Nucl. Phys.* **A605**, 301 (1996)
[8] R Ma, E S Paul, C W Beausang, S Shi, N Xu and D B Fossan, *Phys. Rev.* **C36**, 2322 (1987)
[9] J Gizon, A Gizon, R M Diamond and F S Stephens, *Nucl. Phys.* **A290**, 272 (1977)
[10] R Aryaeinejad, D J G Love, A H Nelson, P J Nolan, P J Smith, D M Todd and P J Twin, *J. Phys. G. Nucl. Phys.* **10**, 955 (1984)
[11] A Galindo-Uribarri, S M Mullins, D Ward, M Cronaz, J DeGraaf, T E Drake, S Flibotte, V P Janzen, D C Radford and I Ragnarsson, *Phys. Rev.* **C54**, R454 (1996)
[12] K Hara and Y Sun, *Int. J. Mod. Phys.* **E4**, 637 (1995)
[13] K Hara and Y Sun, *Nucl. Phys.* **A529**, 445 (1991) and references cited therein
[14] Y Sun and J L Egido, *Nucl. Phys.* **A580**, 1 (1994)
[15] Rani Devi, B D Sehgal and S K Khosa, *Pramana – J. Phys.* **67(3)**, 467 (2006)
[16] Rani Devi, B D Sehgal, S K Khosa and J A Sheikh, *Phys. Rev.* **C72**, 064304 (2005)
[17] B D Sehgal, Rani Devi and S K Khosa, *J. Phys. G: Nucl. Phys.* **32**, 1211 (2006)
[18] T Bengtsson and I Ragnarsson, *Nucl. Phys.* **A436**, 14 (1985)
[19] R A Meyer, E Monnand, J A Pinston, F Schussler, I Ragnarsson, B Pfeiffer, H Lawin, G Lhersonneau, T Seo and K Sistemich, *Nucl. Phys.* **A439**, 510 (1985)
[20] S Goriely, F Tondeur and J Pearson, *At. Data Nucl. Data Tables* **77(2)**, 338 (2001)
[21] O Vogel *et al*, *Phys. Rev.* **C56**, 1338 (1997)
[22] A Bohr and B R Mottelson, *Nuclear Structure*, in: *Nuclear deformations* (World Scientific, Singapore, 1998) Vol. II
[23] T Lönnroth, S Vajda, O C Kistner and M H Rafailovich, *Z. Phys.* **A317**, 215 (1984)
[24] F Dönau and S Frauendorf, in *Proceedings of the Conference on High Angular Momentum Properties of Nuclei*, Oak Ridge, 1982, edited by N R Johnson (Harwood Academic, New York, 1983) p. 143
F Dönau, *Nuc. Phys.* **A471**, 469 (1987)
[25] S Törmäneu *et al*, *Nucl. Phys.* **A572**, 417 (1994)
[26] K Kitao and M Oshima, *Nucl. Data Sheets* **77**, 1 (1996)
[27] Yu Khazov, I Mitropolsky and A Rodinonov, *Nucl. Data Sheets* **107**, 2715 (2006)